



PONTIFICIA UNIVERSIDAD CATOLICA DE CHILE

ESCUELA DE INGENIERIA

ASSESSING THE IMPACT OF TRAVEL TIME FORMULATIONS ON THE PERFORMANCE OF SPATIALLY DISTRIBUTED TRAVEL TIME METHODS

VICENTE ZUAZO

Thesis submitted to the Office of Research and Graduate Studies in partial fulfillment of the requirements for the Degree of Master of Science in Engineering.

Advisor:

JORGE ALFREDO GIRONAS

Santiago de Chile, December, 2013

© 2013, Vicente Zuazo



PONTIFICIA UNIVERSIDAD CATOLICA DE CHILE
ESCUELA DE INGENIERIA

ASSESSING THE IMPACT OF TRAVEL TIME FORMULATIONS ON THE PERFORMANCE OF SPATIALLY DISTRIBUTED TRAVEL TIME METHODS

VICENTE ZUAZO

Members of the Committee:

JORGE A. GIRONAS

CARLOS A. BONILLA

JEFFREY D. NIEMANN

ANDRES GUESALAGA

Thesis submitted to the Office of Research and Graduate Studies in partial fulfillment of the requirements for the Degree of Master of Science in Engineering.

Santiago de Chile, December, 2013

To John Snow,
who knows nothing.

ACKNOWLEDGMENTS

Firstly, I want to thank my family for their unwavering support during my years as an engineering student, and my friends for their concern and invaluable advices.

Also, I must thank the Hydraulics and Environmental Engineering department for the general support and help in this process. I thank my fellow graduate, for their professionalism and camaraderie and for their patience and help. I thank all the professors, particularly Dr. Carlos Bonilla for his help and my advisor, Dr. Jorge Gironás, for his knowledge and teachings, his professional and personal support and for showing me the doors to new life experiences.

In a formal way, I must thank the Chilean FONDECYT program through Grant No. 11090136 and the Arturo Cousiño Lyon Scholarship from the Sociedad de Canales del Maipo.

Finally, I want to thank my girlfriend for her attention, moral support, tolerance and unconditional love, even against all odds.

GENERAL INDEX

	Page
DEDICATORIA	ii
ACKNOWLEDGMENTS	iii
GENERAL INDEX.....	iv
INDEX OF TABLES	vi
INDEX OF FIGURES	vii
RESUMEN.....	ix
ABSTRACT	x
1 INTRODUCTION	1
2 SPATIALLY DISTRIBUTED TRAVEL TIME MODELS	4
2.1 Travel time computation	4
2.2 The U-McIUH model	6
3 KW ANALYTICAL SOLUTION AND NUMERICAL MODEL FOR OVERLAND FLOW	7
3.1 Analytical model	7
3.2 Numerical model	9
4 CASE STUDIES.....	11
4.1 Storm events	11
4.2 Synthetic Unchannelized Subcatchments.....	12
5 RESULTS	13
5.1 Rectangular Plane.....	13

5.1.1	Time of concentration	13
5.1.2	Hydrograph analysis.....	16
5.1.3	Validity of the KW approximation in the SDTT approach.....	20
5.2	Dendritic Subcatchment	25
5.2.1	The cascade and parallel connections	25
5.2.2	Hydrograph analysis.....	28
6	CONCLUSIONS	31
	REFERENCES.....	33

INDEX OF TABLES

Table 1 - Comparison of the MCE values of the U-McIUH model and the formulation that neglects upstream contributions ($\lambda = 0$) for three of the different storm events used in this study (and varying Manning's roughness coefficients n and slopes S).....	28
---	----

INDEX OF FIGURES

Figure 1 - The ratio of τ when λ is included and τ when λ is assumed to be 0, plotted as a function of the actual value of λ	6
Figure 2 - Comparison between the hydrographs from the analytical and numerical models for a constant 20 mm h^{-1} excess rainfall pulse of 30 min duration.	10
Figure 3 - (a) The 100 m by 20 m plane subcatchment when represented with 5 20-m square grid-cells (left) or 2000 1-m square grid-cells (right). (b) The synthetic dendritic subcatchment of 82 cells and its flow configuration.....	13
Figure 4 - Ratio between the time of concentration computed without considering upstream contributions $\tau c''$ to the analytical time of concentration τc as a function of the grid cell resolution Δx used to discretize the plane.....	15
Figure 5 - Comparison between the hydrographs generated by the models for storm event 1 (first row) and storm event 2 (second row) when applied to a sloping plane. The plane's properties are $S = 0.01$ and $n = 0.015$	16
Figure 6 - MCE contour lines using the travel time formulation that considers upstream contributions (top) and neglects upstream contributions (bottom) for different terrain resolutions.....	18
Figure 7 - Comparison of the hydrographs generated by the numerical KW model and the SDTT formulations that consider upstream contributions and neglect them ($\lambda = 0$) for different grid resolutions. Top row considers Huff's storm event and bottom row considers the NRCS storm event.	19
Figure 8 - Regions of slope and Manning's roughness coefficient where the KW approximation loses validity (i.e. $K < 20$, $F > 2$, or $KF^2 < 5$) for planes of length 1, 10, and 100 m, subjected to a excess rainfall of 10 mm h^{-1} . Shaded areas denote regions where the KW approximation fails when the length is 1 m.	21
Figure 9 - Values of K , F , and KF^2 for a plane at equilibrium with a constant 10 mm h^{-1} rain pulse of 1 h duration calculated using the analytical KW solution	

and the U-McIUH with resolutions of 5 m and 20 m.	23
Figure 10 - The two limiting cases of grid cell connectivity and their corresponding expressions of time of concentration; (a) the parallel configuration where all cells contribute flow directly to the most downstream cell, and (b) the cascade configuration where the cells are connected in series.	25
Figure 11 - Computed times of concentration for (a) the parallel flow configuration and (b) the cascade flow configuration when the number of contributing cells is varied (in log scale).	27
Figure 12 - Comparison of hydrographs generated by the numerical model and the SDTT formulations that consider upstream contributions and neglect them ($\lambda = 0$) for different combinations of surface roughness and slope applied to the dendritic catchment. Three storm events were simulated: a constant pulse (top row); Huff's event (middle row); and the NRCS event (bottom row).	28

RESUMEN

Los modelos lluvia-escorrentía son herramientas valiosas para simular la respuesta hidrológica de una cuenca. En años recientes, modelos distribuidos de aguas lluvias han sido desarrollados tales como los modelos de Tiempos de Viaje Distribuidos Espacialmente (o SDTT, por sus siglas en inglés). En estos modelos, los tiempos de viaje del flujo en cada celda son integrados a lo largo de los caminos de flujo para generar el hidrograma a la salida de una cuenca. Algunos aspectos de estos modelos siguen sin clarificarse, incluyendo las implicancias de diferentes formulaciones del tiempo de viaje, el grado en que los modelos SDTT consideran las interacciones entre celdas, el efecto de la resolución espacial y la validez general de los supuestos de la teoría de Onda Cinemática, comúnmente considerada en el desarrollo de estos modelos. En el presente estudio, utilizamos un enfoque analítico así como un modelo SDTT para investigar la importancia de considerar contribuciones desde aguas arriba en el cálculo de los tiempos de viaje del flujo en una celda y su influencia en el cálculo del tiempo de concentración y en la forma del hidrograma. Analizamos además el efecto de la resolución espacial en el desempeño de los modelos SDTT. Finalmente, estudiamos la validez de los supuestos de la teoría de la Onda Cinemática cuando se utiliza un modelo SDTT en un plano. Los resultados muestran que considerar contribuciones desde aguas arriba al calcular tiempo de viaje produce mejores resultados. Resoluciones espaciales más finas perjudican la eficiencia del hidrograma simulado y del tiempo de concentración al usar una expresión de tiempos de viaje que no considera contribuciones desde aguas arriba. Finalmente, los supuestos de Onda Cinemática sí aplican al plano si se consideran contribuciones desde aguas arriba, para un amplio rango de pendientes y coeficientes de rugosidad e independiente de la resolución de las celdas.

Palabras Clave: modelación hidrológica; tiempos de viaje; onda cinemática; resolución; espacialmente distribuidos; laderas.

ABSTRACT

Rainfall-runoff models are valuable tools to simulate the hydrologic response of a watershed. In recent years, Spatially Distributed Travel Time (SDTT) methods have been developed as an alternative to semi-distributed and distributed models. In these methods, the travel times of grid-cells are summed along flow paths and then convoluted to generate the hydrograph at the outlet. Some aspects of these models remain poorly understood, including the implications of different travel time formulations, the extent to which SDTT models take into account the interaction among cells, the effects of grid-cell resolution, and the validity of the kinematic wave (KW) assumptions in this context. In this study, we use an analytical approach as well as a SDTT model to investigate the significance of considering upstream contributions when calculating the travel times of cells and its influence on the computed time of concentration and overall hydrograph shape. We also analyze the effect of terrain resolution on the performance of SDTT models. Lastly, we study the validity of the KW assumptions when SDTT models are applied to a plane. Results show that considering upstream contributions when computing travel times yields much better results. When using a travel time expression that neglects upstream contributions, finer grid cell sizes reduce the accuracy of the time of concentration and the simulated hydrograph. Finally, the KW approximation applies to the plane irrespective of the grid-cell resolution when upstream contributions are considered in the SDTT model for a wide range of slopes and roughness coefficients.

Keywords: hydrologic modeling; travel time; kinematic wave; resolution; spatially distributed; hillslope; upstream contribution.

1 INTRODUCTION

Rainfall-Runoff models are essential for the simulation of the catchment response to rainfall input and the prediction of runoff hydrographs and floods. Lumped models were initially developed for this purpose, in which the spatially-distributed properties characterizing land use, soil types, internal storage, and routing are considered through spatially-averaged parameters. In current practice, hydrological simulation is typically performed using semi-distributed models, in which the basin is divided into subcatchments or hydrologic response units (HRUs) corresponding to homogeneous areas that generate runoff and contribute through overland flow to the drainage system. The subcatchments or HRUs are conceptualized as hydrologic elements in which the upstream runoff formation and concentration is lumped and parameterized in a simple manner. This simplicity is contrasted by the representation of the hydraulics of the channel system, which are described in detail using the St. Venant's equations or their simplifications (Rodriguez et al., 2003). Thus, semidistributed approaches can neglect drainage elements and spatial heterogeneity within the subcatchments that might play an important role in generating and directing flow into the channel system (Gironás et al., 2010; Rodriguez et al., 2003).

The growing availability of digital remote-sensing data and Digital Elevation Models (DEMs) has increasingly motivated the use of distributed terrain information to extract and analyze geomorphic measures and perform distributed hydrological and hydraulic modeling (Martinez et al., 2010; Wilson, 2012). The watershed can be divided into cells with distinct parameter values that represent the spatial variations of hydrologic properties. This information can then be used in sophisticated distributed models to solve continuity and momentum equations (dynamic, diffusive, or kinematic wave equations) in each grid cell, and compute the hydrologic response at the watershed outlet (e.g., Reddy et al., 2007; Shahapure et al., 2011; Velleux et al., 2008; Vieux and Vieux, 2002). Nonetheless, these methods are computationally intensive and require advanced computing stations when dealing with large quantities of data.

An alternative approach is that of the Spatially Distributed Travel Time (SDTT)

methods, which are also known as Spatially Distributed Direct Hydrograph (SDDH) travel time methods (Du et al., 2009; Melesse and Graham, 2004). In this approach, travel times are computed for each grid-cell and summed along flow paths to the outlet. Stormflow at any subcatchment outlet is either determined by the sum of the volumetric flow rates from all contributing cells at each respective travel time (e.g., Buchanan et al., 2012; Buchanan et al., 2013; Chinh et al., 2013; Du et al., 2009; Melesse and Graham, 2004) or the convolution of the excess rainfall and a unit hydrograph computed from the travel times to the outlet (e.g., Ajward, 1996; Gironás et al., 2009; Hall et al., 2001; Kilgore, 1997; Kute and Stuart, 2008; Lee et al., 2008; Maidment, 1993; Muzik, 1996). Although SDTT methods have been shown to succeed in hydrologic modeling and hydrograph computation, there is not a total understanding of the limitations of these methods. Saghafian and Noroozpour (2010) exposed three general issues, particularly when computing travel times on hillslopes. First, the use of flow velocity rather than flood wave celerity in the travel time formulation describes the travel time of a drop of water, which is distinct from the time difference between the occurrence of an elemental effective rainfall at a location and the center of mass of the resulting runoff at the outlet. Second, neglecting the effect of any upstream flow contributions to the cell for which travel time is computed implicitly neglects the fact that hydraulic radius and flow velocity typically increase in the downstream direction, as considered in some existing models (e.g., Maidment et al., 1996; Saghafian et al., 2002). Third, the use of a single map of travel times to compute the movement of water from a location to the outlet for all excess rainfall pulses neglects the fact that rainfall intensity may change as the wave moves downstream. Saghafian and Noroozpour (2010) also pointed out that these issues may produce larger errors in the model results when the area threshold that is used to distinguish channels from hillslopes is large.

These issues and other simplifications associated with SDTT methods have been indirectly addressed to some extent by defining calibration parameters that modify the travel time expression (Du et al., 2010). Additionally, Gironás et al. (2009) hypothesized that these issues can be partially addressed in existing SDTT models by representing the

majority of the flow in the basin using channels, which consider upstream contributions in the travel time formulation. Gironás et al. (2009) also developed and tested the so called Urban Morpho-climatic Instantaneous Unit Hydrograph (U-McIUH) model, which addresses the first and second issues given earlier in a formal way. In particular, the model uses wave celerity based travel time expressions for both channels and hillslopes, which also incorporate the upstream contributing area to the cells. This approach was empirically shown to have a significant positive effect when simulating the timing of observed hydrographs for the specific case study (Gironás et al., 2009). However, there is a need to assess the implications of considering flow accumulation on the travel time formulae in SDTT models in a more general way. Similarly, the effect of the spatial resolution (i.e. grid-cell size) on the accuracy of SDTT results needs to be evaluated.

The objective of this study is to evaluate the benefits and limitations of the different travel time formulae including the related issue of the spatial resolution of the grid. This study will facilitate improved application of this simple distributed approach in hydrologic modeling. The analysis compares four methods that are commonly used to obtain the hydrographs from hillslopes inside a watershed. The first method is the U-McIUH, which uses travel time expressions that depend on rainfall intensity and include upstream flow contributions. The second method is obtained by neglecting upstream flow contributions in the U-McIUH expressions to imitate other existing SDTT methods. The third method is the analytical solution for a kinematic wave (KW) on a plane under constant excess rainfall, and the fourth method is a numerical implementation of complete KW routing in KINEROS2 (Woolhiser et al., 1990). These last two models will be used as the standards against which the two SDTT formulations are judged. Two synthetic unchannelized subcatchments (or hillslopes) will be used: an idealized plane with varying grid resolutions and a small dendritic-like configuration of cells that aims to include the aggregation of flow paths on an irregular hillslope. The models will be compared under four different synthetic storm events: two constant rain pulses (one longer than the catchment's equilibrium time and one shorter), a Huff precipitation event

(Huff, 1967) to simulate time-varying rainfall, and an NRCS event to simulate an event with a more pronounced peak. Special attention will be given to the time of concentration, which should be well approximated by a travel time method if the method is to be successful for more general use. Additionally, for the plane, we study the effects that grid-cell size and flow accumulation have on the assumptions of KW theory, from which the travel time formulations of the U-McIUH model are derived. The outline of this paper is as follows. In the next section, we present the SDTT models and the travel time formulations tested in this study. After that, we present the KW solutions to which the simulations are compared and the case studies. The results of the study are then discussed for each case study, and the key conclusions are summarized at the end.

2 SPATIALLY DISTRIBUTED TRAVEL TIME MODELS

Travel time expressions are a defining characteristic of SDTT models. The expressions are typically based on KW theory, given its suitability to rainfall-runoff modeling in natural and urban catchments (Overton and Meadows, 1976; Singh, 2001; Xiong and Melching, 2005). SDTT methods consider a grid of cells to represent the terrain for hydrologic modeling. Different expressions may be used to compute travel times in different cells, depending on the classification of the cell (e.g., hillslope or channel). These expressions depend on the cell characteristics (e.g., slope, surface roughness, and channel width), excess rainfall intensity, and possible upstream contributions. In this section, we present the travel time formulae considered in this study as well as the U-McIUH. We will focus our analysis on hillslope grid cells for simplicity and because the limitations of SDTT models are potentially more important for these cells than cells representing channels (Saghafian and Noroozpour, 2010).

2.1 Travel time computation

According to the KW theory, the wave-celerity-based travel time τ for a hillslope cell of flow length ℓ and slope S that is subjected to a uniform excess rainfall pulse of intensity E , and a constant upstream inflow per unit width is given by (Wong,

1995):

$$\tau = 6.99 \left(\frac{n\ell}{\sqrt{S}} \right)^{0.6} E^{-0.4} [(\lambda + 1)^{0.6} - \lambda^{0.6}] \quad (1)$$

where n is Manning's roughness coefficient, τ is in min, S in mm^{-1} , ℓ in m, and E in mm h^{-1} . Eq. (1) is an expression for the travel time across the plane of the wave generated at the upstream end of the plane (i.e. the plane's time to equilibrium) that explicitly considers the excess precipitation. The equation includes flow contribution from upstream cells by incorporating λ , which is the ratio of the upstream inflow to the flow generated by the plane due to effective rainfall. If $\lambda = 0$ (i.e. no upstream inflow to the cell is considered), Eq. (1) reduces to the traditional kinematic wave expression for time of equilibrium of a rectangular plane of length ℓ (Viessman and Lewis, 1995). Eq. (1) with $\lambda = 0$ applied to each hillslope grid-cell is the most widely used travel time expression in SDTT modeling (e.g., Buchanan et al., 2012; Chinh et al. 2013; Du et al., 2009; Kilgore, 1997; Kute and Stuart, 2008; Melesse and Graham, 2004), despite the drawbacks previously identified. In this study, we will use Eq. (1) with both $\lambda = 0$ (i.e. neglecting upstream contribution) and $\lambda \neq 0$ (i.e. considering upstream contribution) as travel time expressions. From hereafter, results obtained with both travel time expressions will be referred to as $\lambda = 0$ and U-McIUH, respectively. The last identification is used because the U-McIUH model originally considers this travel time expression. Thus, both expressions account for the effect of the rainfall intensity, but only the U-McIUH takes into account the effect of the upstream contribution. Figure 1 plots the ratio of τ when the upstream contribution is included to τ when this contribution is neglected. If upstream contributions are unimportant to τ , this ratio should remain near one. As λ increases, the ratio drops quickly to values below 0.4, which indicates that the time of equilibrium of the plane is much smaller when upstream contributions are included.

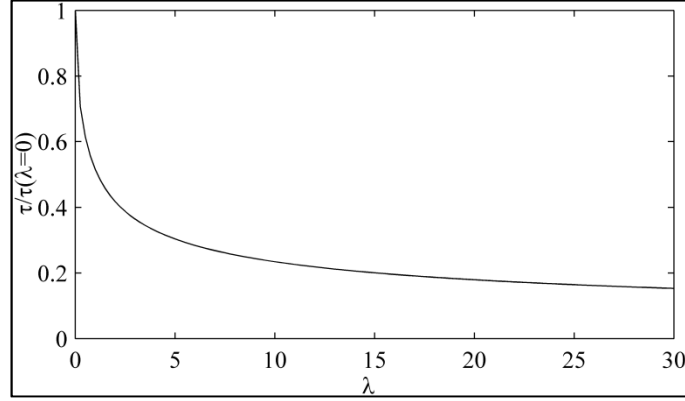


Figure 1 - The ratio of τ when λ is included and τ when λ is assumed to be 0, plotted as a function of the actual value of λ .

2.2 The U-McIUH model

The U-McIUH model (Gironás et al., 2009) is the SDTT method used in this study. Although the current version of the U-McIUH model incorporates several infiltration methods to calculate excess precipitation, in this study, we specify storm events of excess rainfall directly to rule out any effect from infiltration and its modeling. Thus, no infiltration routine is used. Eq. (1) is applied to every hillslope cell in the U-McIUH. Analogous expressions could be used to compute travel times in cells representing channels and pipes, but such cells are not considered in this analysis. In the U-McIUH, the parameter λ is assumed to be constant in time and equal to the ratio of the total effective contributing area to the effective area of the receiving cell. The $\lambda = 0$ case is implemented in the model by directly setting this variable to zero at all locations. For each pulse of excess precipitation, the model calculates the travel time associated with each grid-cell, and then computes the travel time from each grid cell to the outlet using the flow paths calculated from the terrain. The model then computes the IUH associated with each pulse of excess rainfall, which is equivalent to the probability density function (PDF) of the travel times (Rodríguez-Iturbe and Valdés, 1979; Gupta et al., 1980). The outflow for each excess rainfall pulse is determined by the

multiplication of the spatially averaged excess precipitation pulse and the corresponding IUH. Finally, the overall outflow hydrograph is calculated by superimposing the response for each pulse of excess rainfall. Other SDTT models determine the overall outflow hydrograph by adding the volumetric flow rates from all contributing cells at each respective travel time rather than performing a convolution. This difference between methods is not expected to have a strong effect on the results of this study because they are focused on the travel time calculations. Because the IUH's in the U-McIUH are different for different excess rainfall pulses, the model incorporates to some extent the nonlinearity of catchment response, as suggested by Rodríguez-Iturbe et al. (1982). This quasi-linear approach was proposed by Muzik (1996) and has been used by others (e.g., Chinh et al. 2013; Du et al., 2009; Hall et al., 2001; Lee and Yen, 1997; Lee et al., 2008). For more details about the U-McIUH, readers are referred to the original reference for the model (Gironás et al., 2009).

3 KW ANALYTICAL SOLUTION AND NUMERICAL MODEL FOR OVERLAND FLOW

Because SDTT models are approximations of KW routing, analytical solutions and a numerical KW model are used to evaluate these models. For the special case where a constant excess rainfall pulse is applied to a plane with constant slope, analytical KW solutions are available. For other conditions, a numerical method can be used to solve the KW equations (e.g., Gottardi and Venutelli, 2008; Kazezyılmaz-Alhan and Medina, 2007; Singh, 1996).

3.1 Analytical model

The KW equations for a plane are a simplification of the Saint Venant equations and are given by (Lighthill and Witham, 1955):

$$\frac{\partial y}{\partial t} + \frac{\partial q}{\partial x} = E(x, t) \quad (2)$$

$$q = \alpha y^m \quad (3)$$

where y is the flow depth, E the lateral inflow per unit width (i.e. the excess rainfall), t is time, x is the distance downslope measured from the upstream end of the plane, and q is the discharge per unit width. m is the KW exponent and α is the friction parameter, which are assumed constant in space and time for each simulation.

Let's consider a uniform plane with invariant properties and length L in the direction of the flow. Excess rainfall intensity E is assumed to be constant both in time and space, and the initial and boundary conditions are imposed to be:

$$y = 0 \quad \text{if} \quad \begin{cases} 0 \leq x < L & t = 0 \\ x = 0 & t > 0 \end{cases} \quad (4)$$

Eqs. (2) and (3) can be solved using the method of characteristics (Eagleson, 1970), which allows the computation of the flow depth at the end of the plane $y_L = y(t, x = L)$. Then, the discharge hydrograph can be computed from the equation $q_L = \alpha y_L^m$. Two distinct solutions occur depending on the duration of the excess rain pulse T_r , which can be longer or shorter than the time of concentration of the plane τ_c . For $T_r > \tau_c$, y_L is given by (Eagleson, 1970):

$$y_L = \begin{cases} Et & 0 \leq t < \tau_c \\ \left(\frac{LE}{\alpha}\right)^{1/m} & \tau_c \leq t \leq T_r \\ y_L|L = \alpha y_L^{m-1} [y_L E^{-1} + m(t - T_r)] & t > T_r \end{cases} \quad (5)$$

Similarly, for $T_r < \tau_c$, y_L is given by:

$$y_L = \begin{cases} Et & 0 \leq t < T_r \\ ET_r & T_r \leq t \leq t_p \\ y_L|L = \alpha y_L^{m-1} [y_L E^{-1} + m(t - T_r)] & t > t_p \end{cases} \quad (6)$$

where $t_p = T_r(1 - 1/m) + L/\alpha m(ET_r)^{m-1}$ is the time when the recession phase of the hydrograph starts.

An important characteristic of the plane that can be derived from the previous formulae is the time of concentration τ_c . It corresponds to the time at which the catchment or plane is in equilibrium or equivalently the travel time to the downstream end of the plane ($x = L$) of a wave originating at the upstream end of the plane ($x = 0$) (Bedient and Huber, 2002). τ_c is given by (Singh, 1996):

$$\tau_c = \left(\frac{LE^{1-m}}{\alpha} \right)^{1/m} \quad (7)$$

which depends on the rainfall intensity among other variables. Finally, using Manning's equation, values of the friction parameter and the exponent are obtained as $\alpha = \sqrt{S}/n$ and $m = 5/3$, respectively. Then, τ_c is given by the following expression:

$$\tau_c = \left(\frac{nL}{\sqrt{S}} \right)^{0.6} E^{-0.4} \quad (8)$$

which becomes equivalent to Eq. (1) when no upstream contribution occurs if applied to a square grid-cell of length ℓ .

3.2 Numerical model

A numerical model is also used to assess the performance of the different travel time formulations under time-varying excess rainfall. For this purpose we utilized the KINEROS2 model (Woolhiser et al., 1990), a physically based model that solves the KW differential equations of overland flow using a finite difference approach. KINEROS2 is a distributed model in which the catchment is represented

as a cascade of cells or channels. The model was checked by comparing the numerical and analytical solutions for a 20 by 100 m plane under a 10 mm h^{-1} excess rainfall pulse that is larger than the time of concentration (Figure 2). The hydrographs from the analytical and numerical solutions are very similar, although numerical dispersion is observed in the KINEROS2 results when the discharge approaches equilibrium. The continuity error between rainfall and runoff was 0.1%.

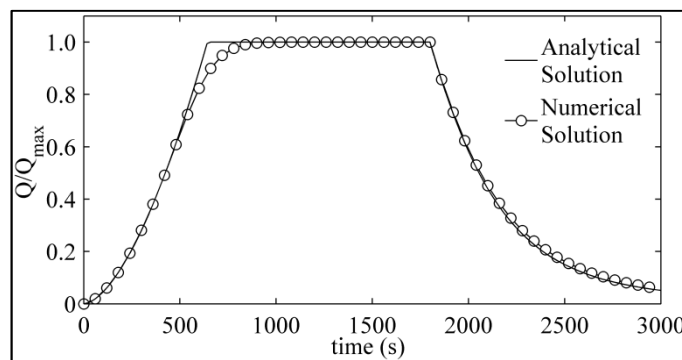


Figure 2 - Comparison between the hydrographs from the analytical and numerical models for a constant 20 mm h^{-1} excess rainfall pulse of 30 min duration.

Because a hillslope cell in KINEROS2 cannot receive contributions from more than one upstream cell, dummy channel elements with nearly zero length were used to sum the hydrographs when two or more upstream cells contribute to a single hillslope cell. To validate this approach, we compared the outflow hydrograph generated by this procedure and by manually adding contributions among cells on a synthetic surface of 16 cells that were randomly connected. Several combinations of roughness, slope, and excess rainfall intensities were used in this comparison. The resulting hydrographs are practically the same, which implies that short dummy channels do not alter the hydrographs from the contributing cells.

4 CASE STUDIES

4.1 Storm events

Four different excess rainfall events are used in this study. Storm event 1 is a 1 h pulse of constant intensity equal to 10 mm h^{-1} and is mainly used to simulate equilibrium conditions. Storm event 2 is a 10 min pulse with a constant intensity of 5 mm h^{-1} and is used to simulate the response to a rain pulse shorter than the time of concentration. The time step used for entering and simulating constant rainfall events was set to 5 min, as this short time step allows representation of rapid changes in the runoff hydrographs (Bedient and Huber, 2002) and is commonly used in hydrologic modeling. It is also approximately the time of concentration of a hillslope cell considering the characteristics (rainfall intensity, slope, roughness and size) adopted later in this study. Thus, the assumption that all cells achieve equilibrium in every rainfall pulse is usually maintained.

Storm event 3 is a first-quartile Huff's rainfall, with a probability level of 50%, in which most of the rain occurs very early within the event (Huff, 1967). This event lasts for 6 h and for simplicity was defined using 10 pulses of 36 minutes each (the coarser time resolution for this event has little effect on the results), also ensuring that grid-cells are able to reach equilibrium for each excess rainfall pulse. A total excess precipitation of 12.7 mm (0.5 in) was used because it is consistent with the long term and large scale averages calculated by Driscoll et al. (1989) for storms in the North Central and Northeast regions of the United States as well as the inland of the West Coast. Finally, storm event 4 corresponds to the widely-used type II, 24-hour NRCS/SCS (National Resources Conservation Service, formerly the Soil Conservation Service) design rainfall event (Bedient and Huber, 2002), with a total depth of 12.7 mm as well and a 1 h time step. This storm allows the assessment of the models' performance under an event with a pronounced peak.

4.2 Synthetic Unchannelized Subcatchments

The models are applied to two synthetic unchannelized subcatchments (or equivalently, hillslopes involving multiple grid cells). The first is a plane of fixed dimensions (100 m length by 20 m width) and constant slope (multiple values are used), which was subdivided into grid cells using different resolutions (1, 5, 10 and 20 m), as illustrated in Figure 3a. In all these representations, the slope and roughness coefficient associated with each cell are always equal to those defined for the plane and are initially set to standard values ($S = 0.01$ and $n = 0.015$). Thus, we can test the performance of the model and travel time expressions under different spatial resolutions in a very simple case for which both numerical and analytical solutions are available.

To test the model in a more realistic environment where aggregation of flow paths occurs, we created a dendritic unchannelized subcatchment of only hillslope cells by following the random aggregation model proposed by Takayasu et al. (1988). This procedure considers a discrete domain of unit mass particles that independently jump to a random location within the domain with a given probability. If two or more particles come together at the same location, their mass is conserved. Then, another set of unit mass particles is injected to the domain and the aggregation process is repeated in time. If the domain is restricted to two dimensions and the particles are restrained to stay on the same site or jump to its closest neighbor with the same probability, the model creates dendritic structures similar to Scheidegger's model of streams (Scheidegger, 1967). The main assumption of the model is that the flow directions tend to occur in a dominant direction (never locally backwards). Thus, this model is more appropriate for representing flow path aggregation on a hillslope with relatively high gradient than the aggregation of streams in a large channelized basin. After creating a series of dendritic structures, we selected a small subcatchment of 82 squared cells (Figure 3b). Each cell is assigned a length of 20 m, a resolution similar to DEMs that are used for distributed hydrological modeling. All cells share the same slope and

surface roughness, firstly set to standard values ($S = 0.01$ and $n = 0.015$).

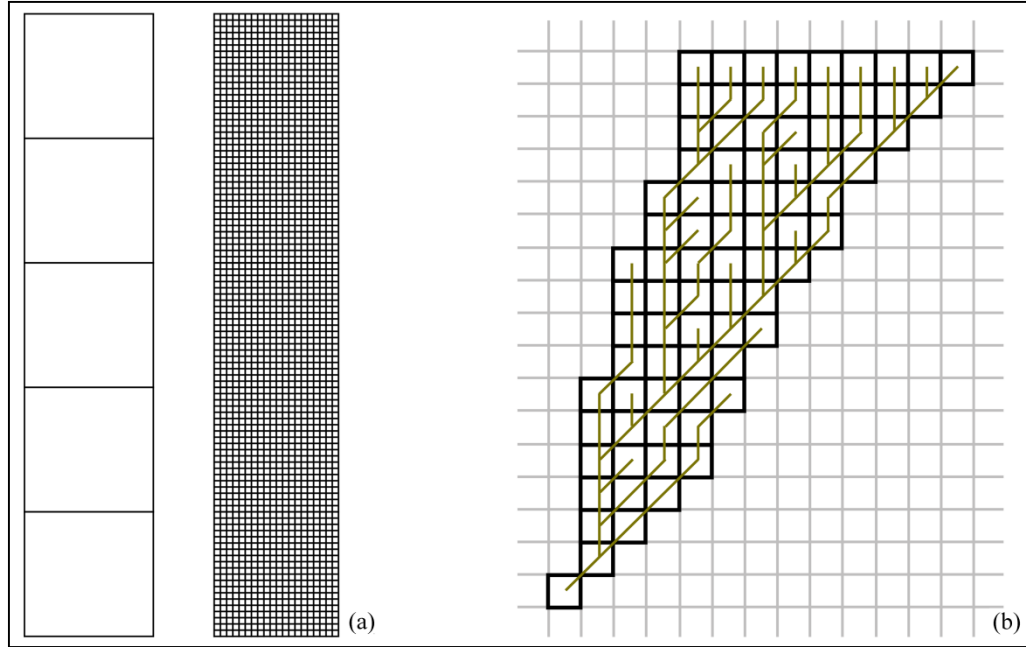


Figure 3 - (a) The 100 m by 20 m plane subcatchment when represented with 5 20-m square grid-cells (left) or 2000 1-m square grid-cells (right). (b) The synthetic dendritic subcatchment of 82 cells and its flow configuration.

5 RESULTS

5.1 Rectangular Plane

We first apply the SDTT model with both travel time expressions to the rectangular plane and compare the simulated responses to those produced by analytical KW solutions. We assess the capacity of these expressions to reproduce both the theoretical time of concentration and outflow hydrographs for different storm events.

5.1.1 Time of concentration

The time of concentration τ_c generated by the SDTT model is a useful way to

compare the travel time formulations. Under the SDTT framework, τ_c is computed as the summation of the travel times along the N cells from the most upstream cell to the most downstream cell. This approach can be used because the travel time associated with each cell is assumed to be that of equilibrium. Here, we consider the case of an impermeable plane of roughness n , slope S , and length L that is represented by a cascade of N hillslope cells of size Δx . If the plane receives a constant excess rainfall intensity E , the time of concentration of the plane τ'_c obtained when considering the travel time expression given by Eq. (1) (i.e. when considering upstream contributions), is computed as:

$$\tau'_c = \sum_{j=1}^N 6.99 \left(\frac{n\Delta x}{\sqrt{S}} \right)^{0.6} E^{-0.4} \left[\left(\frac{A_u}{A} + 1 \right)^{0.6} - \left(\frac{A_u}{A} \right)^{0.6} \right] \quad (9)$$

Since all cells are impermeable, the parameter λ in Eq. (1) reduces to the ratio of upstream contributing area to the area of the cell j , A_u/A . This ratio is then equivalent to the number of upstream cells contributing to the cell, so A_u/A equals zero for the most upstream cell ($j = 1$) and increases by one for each cell along the flow path. Thus, $A_u/A = j - 1$, and Eq. (9) can be rewritten as:

$$\tau'_c = 6.99 \left(\frac{n\Delta x}{\sqrt{S}} \right)^{0.6} E^{-0.4} \sum_{j=1}^N [j^{0.6} - (j-1)^{0.6}] \quad (10)$$

The summation in the last equation equals $N^{0.6}$, which can be written in terms of L and Δx as $N^{0.6} = (L/\Delta x)^{0.6}$. Hence, Eq. (10) becomes:

$$\tau'_c = 6.99 \left(\frac{nL}{\sqrt{S}} \right)^{0.6} E^{-0.4} \quad (11)$$

which is equivalent to the KW time of equilibrium of the entire plane (i.e. Eq. (8)). Thus, the travel time definition of the U-McIUH model (i.e. considering upstream contributions) is robust with respect to the discretization and consistent with KW theory.

Using the travel time expression that neglects the upstream effect on travel time (Eq. (1) with $\lambda = 0$), the time of concentration, referred now as to τ_c'' , can be written as:

$$\tau_c'' = 6.99 \left(\frac{n\Delta x}{\sqrt{S}} \right)^{0.6} E^{-0.4} N = 6.99 \left(\frac{n}{\sqrt{S}} \right)^{0.6} \frac{L}{(E\Delta x)^{0.4}} \quad (12)$$

Thus, τ_c'' in this case depends on the grid-cell size. Moreover, the ratio between Eq. (12) and Eq. (8) is given by:

$$\frac{\tau_c''}{\tau_c} = \left(\frac{L}{\Delta x} \right)^{0.4} \quad (13)$$

Eq. (13) implies that the travel time expression that neglects the upstream contribution increasingly overestimates the time of concentration of the plane as the grid-cell size becomes finer. An application of Eq. (13) using a plane of length $L = 100$ m is shown in Figure 4. A 1 m grid cell size yields a τ_c'' more than 6 times the analytical τ_c . This result is important given that finer resolutions are needed to better represent features of the terrain. Coarser resolutions smooth the catchment topography and lose definition of the hillslopes and channel network (Martinez et al., 2010).

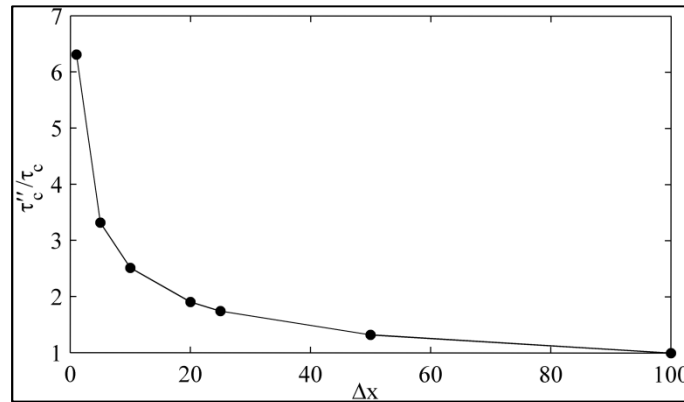


Figure 4 - Ratio between the time of concentration computed without considering upstream contributions τ_c'' to the analytical time of concentration

τ_c as a function of the grid cell resolution Δx used to discretize the plane.

5.1.2 Hydrograph analysis

The previous analysis can be expanded to understand how the hydrographs produced by different travel time expressions under different resolutions compares to analytical solutions (Figure 5). A constant slope $S = 0.01$ and a Manning's roughness $n = 0.015$, which is typical of asphalt or concrete paving (Bedient and Huber, 2002), were selected as a base case. Considering storm event 1, Eq. (8) yields a time of concentration of 14.13 min. The U-McIUH model is able to represent this time of concentration and the overall shape of the hydrograph irrespective of the resolution (Figure 5, first row). However, the recession limb of the U-McIUH hydrograph is shorter than the analytical and numerical KW solutions. Neglecting upstream contributions on the calculations of travel time yields an overestimated time of concentration, an effect that is aggravated as the cell size is reduced (consistent with Eq. (13)). Moreover, at a resolution of 1 m the simulated hydrograph neither predicts the correct maximum discharge nor the correct timing for reaching the peak discharge, as the computed time of concentration (89 min from Eq. (12)) is longer than the 60 min duration of the event.

Using storm event 2, we can study the behavior of the different travel time formulations under an event that is shorter than the plane's time of concentration (Figure 5, second row). Even when accounting for upstream contributions, the SDTT model is unable to represent the constant maximum outflow generated by the KW theory. A pronounced peak flow is observed and the duration of the discharge hydrograph is shorter for all grid-cell sizes. This difference is due to the fact that the SDTT model assumption of equilibrium in all grid-cells is not true in those near the downstream end of the plane. Neglecting upstream contributions yields a longer duration of the hydrograph and a smaller maximum outflow than the analytical solution. Moreover, increasing the grid-cell size decreases the

duration and increases maximum discharge. Indeed, both travel time formulae behave better for coarser resolutions because the number of cells that are not in equilibrium reduces, and therefore, the assumption of equilibrium for all the cells becomes less harmful.

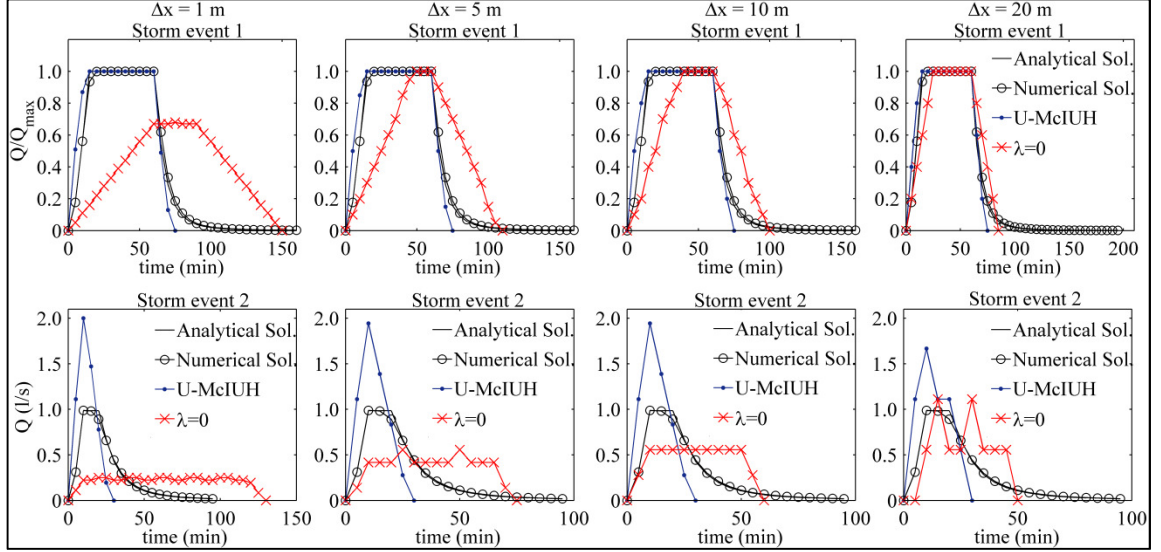


Figure 5 - Comparison between the hydrographs generated by the models for storm event 1 (first row) and storm event 2 (second row) when applied to a sloping plane. The plane's properties are $S = 0.01$ and $n = 0.015$.

To assess the goodness of fit between the models and the analytical solution, we used the modified coefficient of efficiency (MCE), which is defined as (Legates and McCabe, 1999):

$$\text{MCE} = 1 - \frac{\sum_v |Q_{ref,v} - Q_{sim,v}|}{\sum_v |Q_{ref,v} - \bar{Q}_{ref,v}|} \quad (14)$$

where v indicates each time step of the simulation period, $Q_{sim,v}$ is the simulated discharge, $Q_{ref,v}$ is the reference discharge given by the analytical solution, and $\bar{Q}_{ref,v}$ is its corresponding average. A MCE value of 1 indicates a perfect match between the reference and simulated discharges, whereas a value of zero means

that the simulation is as good as the average of the reference data.

MCE values associated with both travel time formulations were calculated for the synthetic plane under storm event 1 when varying both the surface roughness ($0.01 \leq n \leq 0.1$) and the slope of the plane ($0.001 \leq S \leq 0.1$) (Figure 6). Considering upstream contributions in the travel times consistently generates better results than those obtained when upstream contributions are neglected. Furthermore, as cell size is reduced the latter yields much worse results. A similar reduction in the MCE values at finer resolutions is also observed for the U-McIUH results but to a much lesser extent. Worse performance for finer resolutions with both models is explained by the increasing number of cells (i.e. travel times) used to build the histograms of travel times, causing more noisy unit hydrographs. Additionally, when $\lambda = 0$, the inconsistency in the travel time expression increasingly affects the unit hydrograph when the total number of cells increases, further decreasing MCE values. Increasing S and/or decreasing n yields better results for both formulations. This behavior is expected because these changes decrease the storage capacity and the travel time on each grid-cell, causing the reduction of the overall differences between models. Note that for mild slope and high roughness combinations, a cell may not reach equilibrium during the 5 min time step used in the analysis. This last issue becomes more relevant for the U-McIUH formulation in those cells whose time of concentration tend to be large (i.e. cells with minor upstream contributions and when large grid-cells sizes are used).

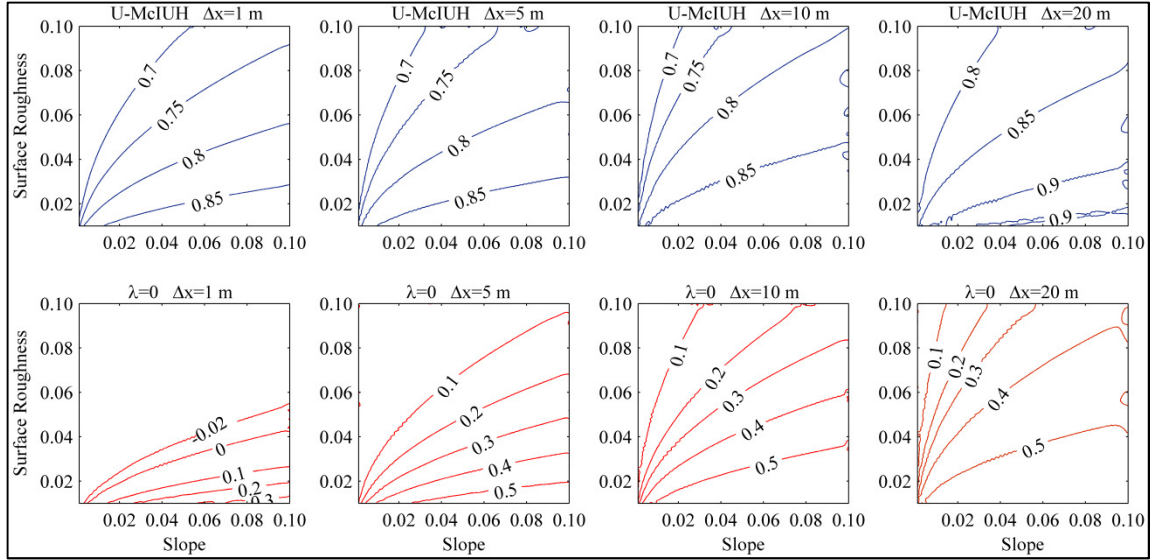


Figure 6 - MCE contour lines using the travel time formulation that considers upstream contributions (top) and neglects upstream contributions (bottom) for different terrain resolutions.

We further analyzed the performance of the travel time formulations for the plane by using the time-varying storm events 3 and 4 (Figure 7, first and second row, respectively). The U-McIUH model (which considers upstream contributions) is capable of reproducing both the time and the value of the maximum discharge from the numerical KW solution irrespective of the cell size. On the other hand, neglecting upstream contributions yields a decreasing maximum flow as the resolution becomes finer. Moreover, the time to peak increases when using a resolution of 1 m, which results in the loss of the hydrograph shape. Other tests show that the effect of increasing n and/or decreasing S is similar to what was reported for storm event 1 in terms of the efficiency with which hydrographs from the numerical solutions are reproduced.

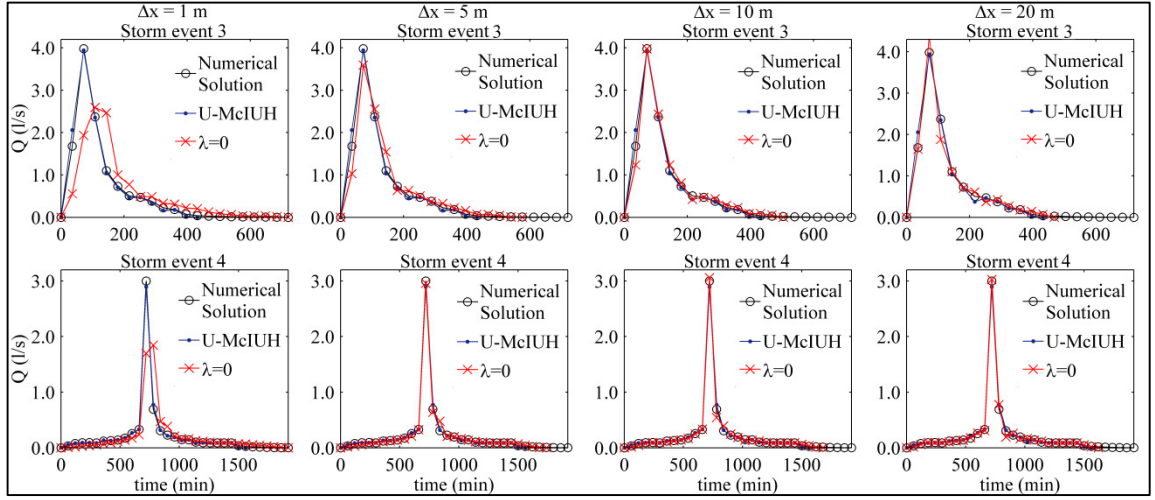


Figure 7 - Comparison of the hydrographs generated by the numerical KW model and the SDTT formulations that consider upstream contributions and neglect them ($\lambda = 0$) for different grid resolutions. Top row considers Huff's storm event and bottom row considers the NRCS storm event.

5.1.3 Validity of the KW approximation in the SDTT approach

The KW equations are known for their simplicity in comparison to the full dynamic wave equations, but they should be used only when certain criteria are met. Ponce (1991) extensively discussed the validity of the KW approach and stated that most shallow overland flows satisfy the criteria needed. Stream flow, on the other hand, usually satisfies the diffusive wave criteria. We now test the validity of the KW approximation when it is applied to compute the travel times in the grid cells of a SDTT model.

Woolhiser and Liggett (1967) derived a locus where the KW approximation holds using the KW number K , which depends on the Froude number F . Considering the downstream end of a sloping plane and assuming that the flow's cross-section is wide and rectangular, K is given by:

$$K = \frac{S L}{y F^2} \quad (15)$$

where:

$$F = \frac{V}{\sqrt{gy}} \quad (16)$$

and S is the slope of the plane, g is gravitational acceleration, V is the flow velocity, and y is the water depth. L is the flow length of the plane without upstream contributions, defined as the distance from the upstream end where $y = 0$ to the point of interest. Both V and y are calculated for the maximum flow at the point of interest. Woolhiser and Liggett (1967) concluded that the KW approximation is valid if $K > 20$. Morris and Woolhiser (1980) later demonstrated that the validity of the KW approximation is also affected by the parameter KF^2 , which corresponds to the ratio of the total height drop of the plane SL and the flow depth y at the downstream end:

$$KF^2 = \frac{SL}{y} \quad (17)$$

Thus, KF^2 increases as the water depth decreases. For $F \leq 0.4$, the KW assumptions are valid only if $KF^2 > 5$, regardless of the value of K (Morris and Woolhiser, 1980). Daluz-Vieira (1983) later demonstrated that the KW approximation also requires that $F < 2$. Supercritical flows with $F > 2$ are associated with highly inertial flows, for which the full momentum equation must be considered.

A plane in equilibrium under a pulse of constant excess precipitation E (with no flow contributions from upstream cells) has explicit solutions for both the velocity and water depth at the downstream end (Eq. (5)). Thus, K , F , and KF^2 are given by:

$$K = gn \left(\frac{LS^2n}{E^4} \right)^{1/5} \quad (18)$$

$$F = \frac{\sqrt{S}}{n\sqrt{g}} \left(\frac{ELn}{\sqrt{S}} \right)^{1/10} \quad (19)$$

$$KF^2 = SL^{2/5} \left(\frac{\sqrt{S}}{En} \right)^{3/5} \quad (20)$$

As L increases, both K and KF^2 increase, which strengthens the validity of the KW approximation. However, F also increases, which weakens the validity of the KW approximation. Thus, larger values of L produce a trade-off in these criteria. Similar trade-offs occur as S increases and n decreases. To illustrate these criteria, Eqs. (18), (19), and (20) were applied to a single grid-cell of length 1 m (Figure 8). The cell was subjected to a constant 10 mm h⁻¹ rain pulse and has no contribution from upstream cells. In this analysis, S and n were allowed to vary 0.001 – 0.1 and 0.005 – 0.5, respectively. Shaded areas in Figure 8 denote S and n combinations where the KW approximation does not hold. L was also increased to 10 m and 100 m and the results are plotted with dashed lines in Figure 8. For larger grid cells, the sizes of the invalid regions associated with KF^2 and F decrease and increase, respectively. The size of the invalid region associated with K is zero in all cases shown. Overall, as the length of the plane increases, the region of KW validity increases.

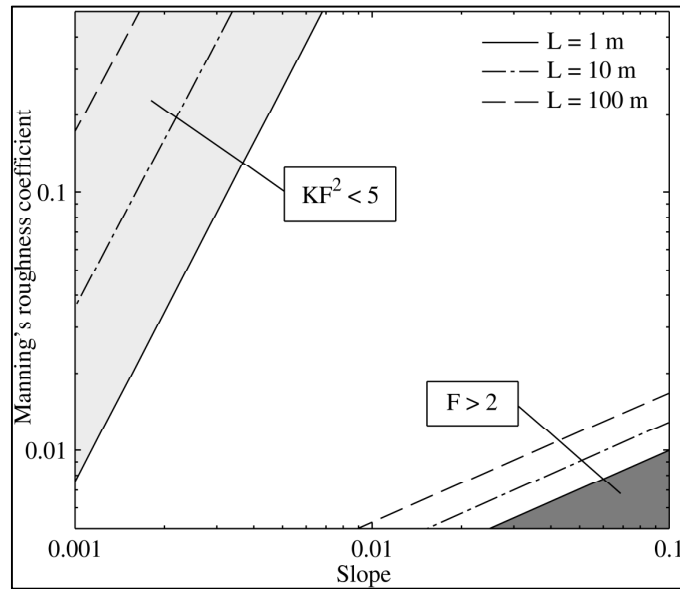


Figure 8 - Regions of slope and Manning's roughness coefficient where the KW approximation loses validity (i.e. $K < 20$, $F > 2$, or $KF^2 < 5$) for planes of length 1, 10, and 100 m, subjected to a excess rainfall of 10 mm h^{-1} . Shaded areas denote regions where the KW approximation fails when the length is 1 m.

The critical parameters K , F , and KF^2 can also be used to evaluate the validity of the KW approximation when the U-McIUH model is applied to a discretized planar hillslope. First, analytical solutions for all three parameters can be obtained for all points on the plane because any point corresponds to the downstream end of an embedded plane. As one considers points further downslope, the length of the embedded plane increases. Thus, F increases, which reduces the validity of the KW approximation. Simultaneously, K and KF^2 increase, which improve the validity of the KW approximation. This analysis can be repeated when the flow velocity and depth are calculated using the U-McIUH. In this case, the plane is discretized using grid-cell sizes of 5 m and 20 m, and K , F , and KF^2 are computed for each cell of the flow path using Eqs. (15), (16) and (17). The U-McIUH model and the analytical solutions yield the same flow velocity and depth for every grid cell on the plane. Thus, K , F , and KF^2 at the downstream end of each cell are the

same for both the analytical solution and the U-McIUH. Different grid-cell sizes exhibit no differences in the values of the parameters at a given flow length.

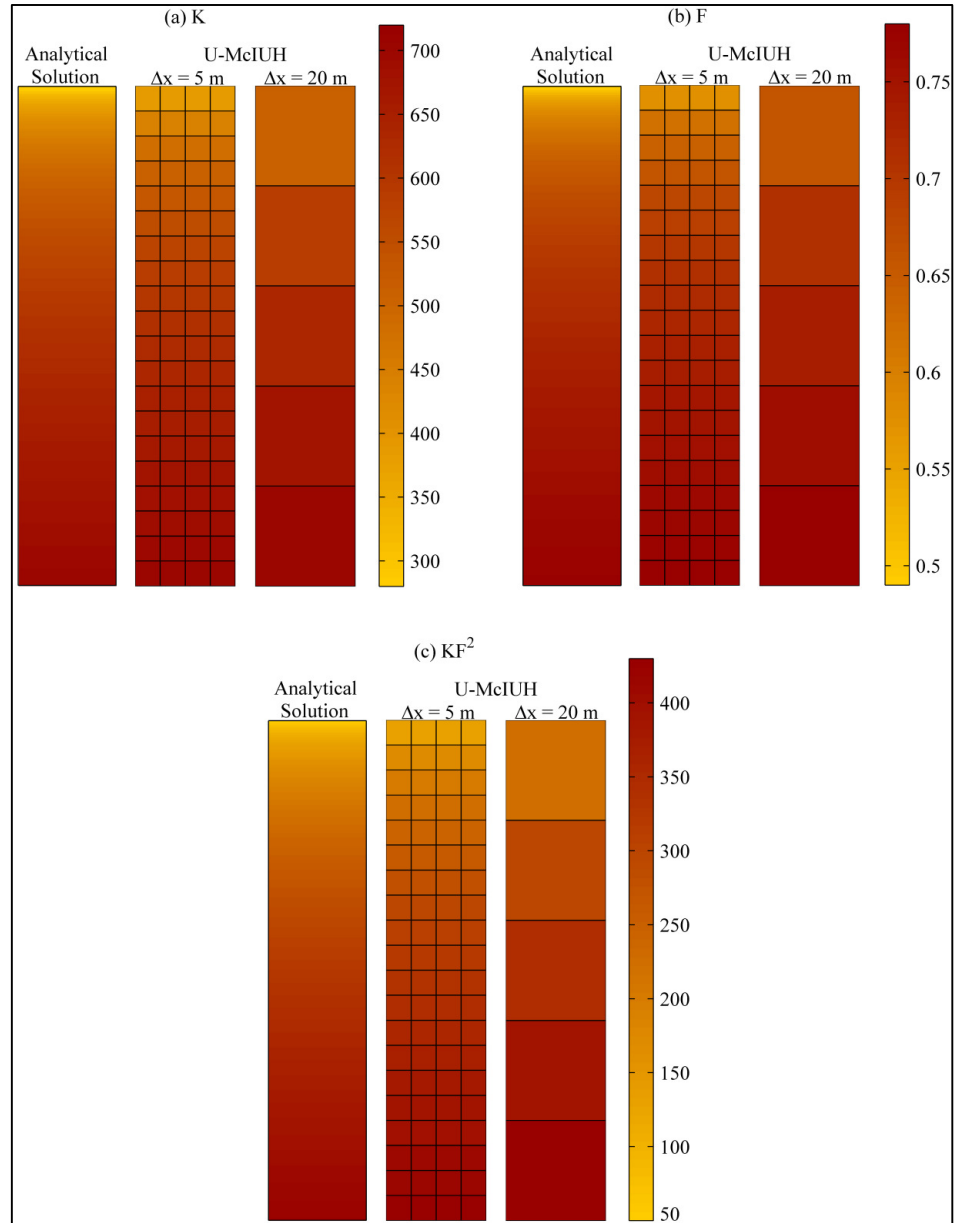


Figure 9 - Values of K , F , and KF^2 for a plane at equilibrium with a constant 10 mm h^{-1} rain pulse of 1 h duration calculated using the analytical KW solution and the U-McIUH with resolutions of 5 m and 20 m.

5.2 Dendritic Subcatchment

Next, we assess the performance of the travel time formulations using the dendritic subcatchment. The dendritic configuration allows grid cells to connect in a more complex manner with some cells receiving flow from more than one upslope cell. Such a configuration is more representative of natural and urban subcatchments than a simple plane.

5.2.1 The cascade and parallel connections

Before considering the complex dendritic configuration, we first study two limiting cases with respect to flow path organization. The first case consists of N equal cells connected in parallel to a downstream cell (Figure 10a). Although a DEM with no pits can have no more than 5 cells draining directly into a cell, we will allow values of N larger than 5 in this theoretical analysis. The second case consists of N equal cells connected in series to a downstream cell (Figure 10b). The latter case is equivalent to the synthetic plane used previously if only a single cascade of cells is considered. In the first case, the time of concentration can be found analytically as the sum of the travel time of the downstream cell and the travel time of one of the upstream cells. The downstream cell has an upstream contribution of N cells, and thus $\lambda = N$. In the second case, the time of concentration is given by the sum of the travel times of each cell in the cascade and the analytical time of concentration is found from Eq. (10).

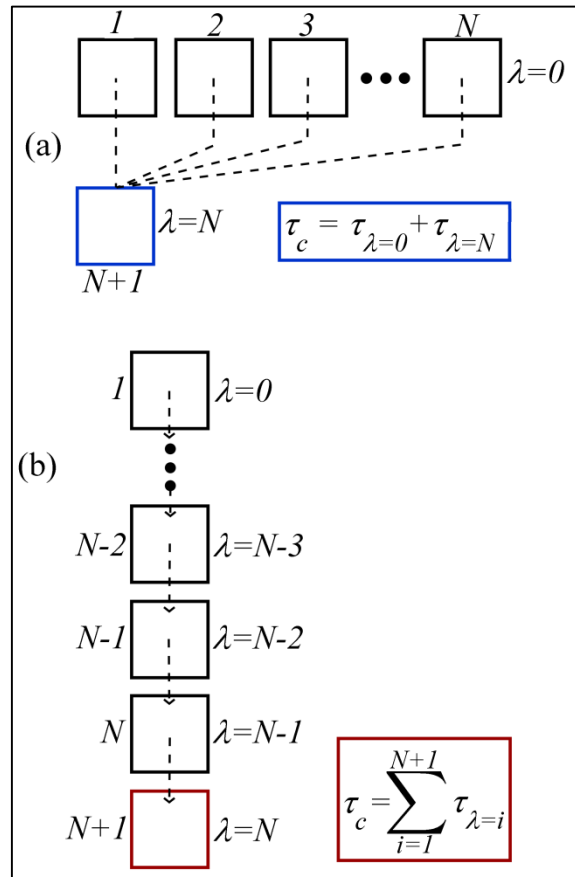


Figure 10 - The two limiting cases of grid cell connectivity and their corresponding expressions of time of concentration; (a) the parallel configuration where all cells contribute flow directly to the most downstream cell, and (b) the cascade configuration where the cells are connected in series.

We compared the time of concentration from the U-McIUH when upstream contributions are included and when they are neglected to these analytical solutions and to the times of concentration calculated by the numerical KW model (Figure 11). We used a 10 mm h^{-1} excess rainfall pulse of infinite duration, a roughness $n = 0.015$, and a slope $S = 0.01$. The grid-cell size was set to 10 m.

For the parallel configuration (Figure 11a), the analytical time of concentration smoothly decreases as the number of upstream cells increases, but its value is typically around 5 min. The times of concentration for the models change abruptly

by increments of 5 min because that is the time step that was used. The U-McIUH model computes a time of concentration of 10 min when $N = 2$ and a time of concentration of 5 min when $N > 2$. The model neglecting upstream contributions has no change in the time of concentration (it is always 10 min) because the travel time in the downstream grid cell remains unchanged as more upstream cells are added. The numerical model behaves similar to the U-McIUH, but a 5 min time shift is observed, which is due to the numerical dispersion previously discussed (see Figure 3).

In the cascade configuration (Figure 11b), the formulation accounting for upstream contributions is consistent with the analytical solution, whereas the same time shift is observed for the numerical model. When upstream contributions are neglected, the time of concentration increases with the number of cells at a rate that is higher than the analytical solution. This result is explained by the fact that no reduction in the travel time occurs in a cell as the number of upstream cells increase.

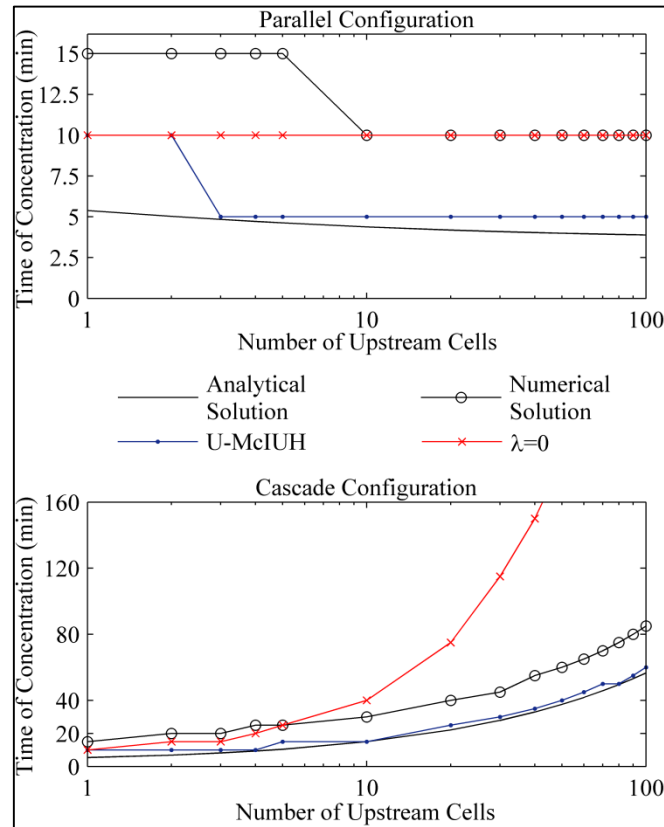


Figure 11 - Computed times of concentration for (a) the parallel flow configuration and (b) the cascade flow configuration when the number of contributing cells is varied (in log scale).

5.2.2 Hydrograph analysis

We now consider the response of the dendritic subcatchment to storm events 1, 3 and 4 (Figure 12 row 1, 2, and 3, respectively) when different values are used for n and S . Considering upstream contributions replicates the maximum flow under the constant rain pulse (storm event 1) when $n = 0.015$ and $S = 0.01$ (Figure 12b), although there are differences in the recession part of the hydrograph and in the time of concentration due to numerical dispersion in KINEROS2 (as shown in Figure 3). Neglecting upstream contributions yields worse results. The overall shape of the hydrograph is lost, and the catchment does not reach equilibrium. If n

is increased and/or S is reduced until the catchment does not reach equilibrium (Figure 12a), both the time to peak and the maximum flow are not well represented irrespective of whether upstream contributions are considered. In contrast, smaller n and larger S values lead to better results for both models (Figure 12c). Overall, neglecting upstream contributions yields worse results.

Similar results are obtained when simulating storm events 3 and 4. When upstream contributions are included, the U-McIUH simulates the time to peak relatively well, but it overestimates the maximum outflow (Figure 12d to Figure 12i), particularly when n is large and S is small. The formulation that neglects upstream contributions is incapable of representing either of those characteristics even for a moderate roughness and slope. Moreover, the shape of the hydrograph is lost for large n and small S (Figure 12d and Figure 12g). As with the constant event, differences lessen for smaller values of n and larger values of S (Figure 12f and Figure 12i).

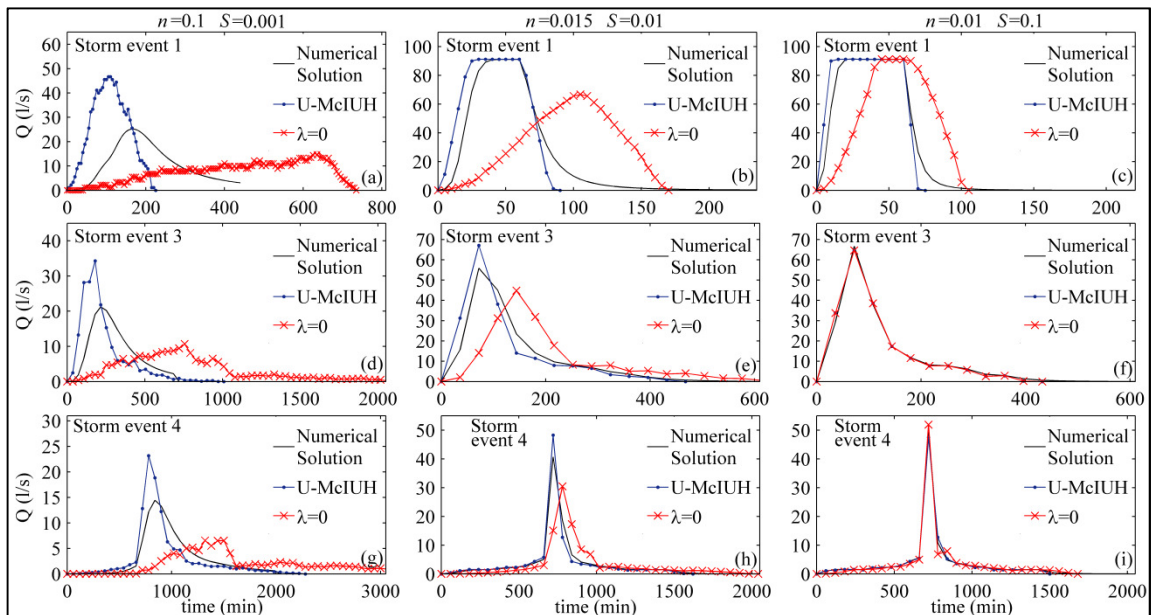


Figure 12 - Comparison of hydrographs generated by the numerical model and the SDTT formulations that consider upstream contributions and neglect them ($\lambda = 0$) for different combinations of surface roughness and slope applied to

the dendritic catchment. Three storm events were simulated: a constant pulse (top row); Huff's event (middle row); and the NRCS event (bottom row).

Table 1 shows the MCE values obtained when comparing the hydrographs from the U-McIUH and the $\lambda = 0$ travel time formulation against those from the numerical KW model. Efficiency drops drastically if the $\lambda = 0$ formulation is used, especially when considering large roughness coefficients and small slopes (i.e. when the storage capacity of each grid-cell increases). In the worst cases, MCE values become negative, meaning that the $\lambda = 0$ model represents the hydrograph from the numerical KW model with less efficiency than the numerical model's average. On the other hand, the performance of the U-McIUH is much more robust for the range of n and S values analyzed.

Table 1 - Comparison of the MCE values of the U-McIUH model and the formulation that neglects upstream contributions ($\lambda = 0$) for three of the different storm events used in this study (and varying Manning's roughness coefficients n and slopes S).

Storm event	Manning's n	U-McIUH			$\lambda = 0$		
		$S = 0.001$	$S = 0.01$	$S = 0.1$	$S = 0.001$	$S = 0.01$	$S = 0.1$
1	0.01	0.55	0.69	0.74	-0.25	-0.20	0.19
	0.015	0.47	0.65	0.73	-0.25	-0.23	0.03
	0.1	-0.92	0.13	0.55	-0.28	-0.24	-0.25
3	0.01	0.57	0.79	0.94	0.30	0.50	0.78
	0.015	0.62	0.68	0.92	0.27	0.38	0.62
	0.1	0.28	0.50	0.57	0.08	0.24	0.30
4	0.01	0.62	0.89	0.93	0.15	0.44	0.84
	0.015	0.60	0.81	0.96	0.03	0.24	0.74
	0.1	0.53	0.64	0.62	-0.30	-0.14	0.15

6 CONCLUSIONS

In this paper, we studied in detail two travel time formulations that can be used in SDTT models. One considers the effect of upstream contributions of flow (the U-McIUH formulation) whereas the other does not. Results associated with these formulations were compared against those generated by analytical solutions and a numerical model that explicitly routes discharge using the KW equations. In this comparison, we used various rainfall events on sloping planes and synthetic unchannelized subcatchments. Based on this comparison, we make the following conclusions:

1. When upstream contributions are neglected in the travel time formulation, the time of concentration is heavily dependent on the grid-cell size. In particular, the time of concentration for a planar hillslope increases as grid-cell size decreases. When considering upstream contributions in the formulation, the time of concentration is independent of the spatial resolution and equal to the analytical time of concentration from KW theory.
2. When considering analytical solutions for a planar hillslope, the KW approximation applies for a wide range of slopes and roughness coefficients, but the validity generally decreases as the length of the hillslope (or contributing area) increases. These analytical limitations are reproduced by the U-McIUH when upstream flow contributions are considered, and they are independent of the grid-cell size that is used in the model.
3. Including upstream contributions when computing travel times also simulates maximum outflow and time to peak for various storm events (i.e. Huff and NRCS storm events) more accurately, and the overall shape of the hydrograph is maintained for both the sloping plane and the unchannelized dendritic subcatchment. For both synthetic catchments, the results of the full KW equations are reproduced more efficiently when using the U-McIUH formulation than using the formulation that neglects upstream contributions. In both cases, efficiency drops with finer resolutions, although this reduction is much more significant when upstream contribution are neglected. Finally, both travel time formulae yield

worse results with increasing surface roughness and/or decreasing slope (i.e. when the storage in the subcatchment increases).

Overall, the results demonstrate that SDTT methods which incorporate upstream contributions in their travel time formulation are more robust and representative of the hydrographs obtained both analytically and with a model that numerically solves the KW equations. This analysis considered only flow on hillslopes, and thus a study of the validity of the KW assumptions in channelized elements within the SDTT framework is advised as future research.

REFERENCES

- Ajward, M.H. (1996). *A spatially distributed unit hydrograph model using a geographical information system*. Ph.D. Dissertation, Civil Engineering Dept. University of Calgary, Calgary.
- Bedient, P.B. and Huber, W.C. (2002). *Hydrology and Floodplain Analysis*, 3rd ed.
- Buchanan, B., Easton, Z.M., Schneider, R. and Walter, M.T. (2012). Incorporating variable source area hydrology into a spatially distributed direct runoff model. *Journal of the American Water Resources Association*, 48 (1), 43-60.
- Buchanan, B.P., Archibald, J.A., Easton, Z.M., Shaw, S.B., Schneider, R.L. and Walter, M.T. (2013). A phosphorus index that combines critical source areas and transport pathways using a travel time approach. *Journal of Hydrology*, 486, 123-135.
- Chinh, L., Iseri, H., Hiramatsu, K., Harada, M. and Mori, M. (2013). Simulation of rainfall runoff and pollutant load for Chikugo River basin in Japan using a GIS-based distributed parameter model. *Paddy and Water Environment*, 11 (1-4), 97-112.
- Daluz-Vieira, J.H. (1983). Conditions governing the use of approximations for the Saint-Venant equations for shallow surface water flow. *Journal of Hydrology*, 60 (1-4), 43-58.
- Driscoll, E.D., Palhegyi, G.E. and Strecker, E.W., Shelley, P.E. (1989). *Analysis of storm event characteristics for selected rainfall gages throughout the United States*. US Environmental Protection Agency, Washington, DC.
- Du, J., Xie, H., Hu, Y., Xu, Y. and Xu, C.Y. (2009). Development and testing of a new storm runoff routing approach based on time variant spatially distributed travel time method. *Journal of Hydrology*, 369 (1-2), 44-54.
- Du, J., Xie, H., Hu, Y., Xu, Y. and Xu, C.Y. (2010). Reply to comment on “Development and testing of a new storm runoff routing approach based on time variant spatially distributed travel time method” by Du et al. [*Journal of Hydrology*, 369 (2009) 44–54]. *Journal of Hydrology*, 381 (3-4), 374-376.
- Eagleson, P.S. (1970). *Dynamic Hydrology*, New York, McGraw-Hill Inc., 1970
- Gironás, J., Niemann, J.D., Roesner, L.A., Rodriguez, F. and Andrieu, H. (2009). A morpho-climatic instantaneous unit hydrograph model for urban catchments based on the kinematic wave approximation. *Journal of Hydrology*, 377 (3-4), 317-334.
- Gironás, J., Niemann, J.D., Roesner, L.A., Rodriguez, F. and Andrieu, H. (2010).

- Evaluation of methods for representing urban terrain in storm-water modeling. *Journal of Hydrologic Engineering*, 15 (1), 1-14.
- Gottardi, G. and Venutelli, M. (2008). An accurate time integration method for simplified overland flow models. *Advances in Water Resources*, 31 (1), 173-180.
- Gupta, V.K., Waymire, E. and Wang, C.T. (1980). A representation of an instantaneous unit hydrograph from geomorphology. *Water Resources Research*, 16 (5), 855-862.
- Hall, M.J., Zaki, A.F. and Shahin, M.M.A. (2001). Regional analysis using the Geomorphoclimatic Instantaneous Unit Hydrograph. *Hydrology and Earth System Sciences*, 5 (1), 93-102.
- Huff, F.A. (1967). Time distribution of rainfall in heavy storms. *Water Resources Research*, 3 (4), 1007-1019.
- Kazezyilmaz-Alhan, C.M. and Medina M. Jr. (2007). Kinematic and diffusion waves: Analytical and numerical solutions to overland and channel flow. *Journal of Hydraulic Engineering*, 133 (2), 217-228.
- Kilgore, J.L. (1997). *Development and evaluation of a GIS-based spatially distributed unit hydrograph model*. MS Thesis, Virginia Polytechnic Institute and State University Blacksburg, VA. p. 118.
- Kute, A. and Stuart, N. (2008). Predicting GIS-based Spatially Distributed Unit Hydrograph from Urban Development Scenarios. *WaPUG Spring Meeting*, June 2008, Coventry, UK.
- Lee, K.T. and Yen, B.C. (1997). Geomorphology and kinematic-wave-based hydrograph derivation. *Journal of Hydraulic Engineering*, 123 (1), 73-80.
- Lee, K.T., Chen, N.C. and Chung, Y.R. (2008). Derivation of variable IUH corresponding to time-varying rainfall intensity during storms. *Hydrological Sciences Journal*, 53 (2), 323-337.
- Legates, D.R. and McCabe Jr., G.J. (1999). Evaluating the use of “goodness-of-fit” measures in hydrologic and hydroclimatic model validation. *Water Resources Research*, 35 (1), 233-241.
- Lighthill, M.J. and Whitham, G.B. (1955). On kinematic waves. I. Flood movement in long rivers. *Proceedings of the Royal Society of London. Series A, Mathematical and Physical Sciences*, 229, 281-316.
- Maidment, D.R. (1993). Developing a spatially distributed unit hydrograph by using

GIS. In: Kovar, K., Nachtnebel, H.P. (Eds.), *Application of Geographic Information Systems in Hydrology and Water Resources*, Proceedings of the Vienna Conference, 211. *IAHS Publ.*, Vienna, pp. 181-192.

Maidment, D.R., Olivera, F., Calver, A., Eatherall, A. and Fraczek, W. (1996). Unit hydrograph derived from a spatially distributed velocity field. *Hydrological Processes*, 10 (6), 831–844.

Martinez, C., Hancock, G.R., Kalma, J.D., Wells, T. and Boland, L. (2010). An assessment of digital elevation models and their ability to capture geomorphic and hydrologic properties at the catchment scale. *International Journal of Remote Sensing*, 31 (23), 6239-6257.

Melesse, A.M. and Graham, W.D. (2004). Storm runoff prediction based on a spatially distributed travel time method utilizing remote sensing and GIS. *Journal of the American Water Resources Association*, 40 (4), 863-879.

Morris, E. and Woolhiser, D. (1980). Unsteady one-dimensional flow over a plane: Partial equilibrium and recession hydrographs. *Water Resources Research* 16 (2), 355-360.

Muzik, I. (1996). Flood modelling with GIS-derived distributed unit hydrographs. *Hydrological Processes*, 10 (10), 1401-1409.

Overton, D.E. and Meadows, M.E. (1976). *Stormwater Modeling*. Academic Press Inc., New York. p. 358.

Ponce, V.M. (1991). The Kinematic Wave Controversy. *Journal of Hydraulic Engineering*, 117 (4), 511–525.

Reddy, K.V., Eldho, T.I., Rao, E.P. and Hengade, N. (2007). A kinematic-wave-based distributed watershed model using FEM, GIS and remotely sensed data. *Hydrological Processes*, 21 (20), 2765–2777.

Rodriguez, F., Andrieu, H. and Creutin, J.D. (2003). Surface runoff in urban catchments: morphological identification of unit hydrographs from urban databanks. *Journal of Hydrology*, 283 (1-4), 146-168.

Rodríguez-Iturbe, I. and Valdés J.B. (1979). Geomorphologic structure of hydrologic response. *Water Resources Research*, 15 (6), 1409-1420.

Rodríguez-Iturbe, I., González-Sanabria, M. and Bras, R.L. (1982). A geomorphoclimatic theory of the instantaneous unit hydrograph. *Water Resources Research*, 18 (4), 877-886.

Saghafian, B, Julien, P.Y. and Rajaie, H. (2002). Runoff hydrograph simulation based on time variable isochrone technique. *Journal of Hydrology*, 261 (1-4), 193–203.

Saghafian, B. and Noroozpour, S. (2010). Comment on “Development and testing of a new storm runoff routing approach based on time variant spatially distributed travel time method” by Jinkang Du, Hua Xie, Yujun Hu, Youpeng Xu, Chong-Yu Xu. *Journal of Hydrology*, 381 (3-4), 372-373.

Scheidegger, A.E. (1967). A stochastic model for drainage patterns into an intramontane treinch. *International Association of Scientific Hydrology*. Bulletin 12 (1), 15-20.

Shahapure, S.S., Eldho, T.I. and Rao, E.P. (2011). Flood Simulation in an Urban Catchment of Navi Mumbai City with Detention Pond and Tidal Effects Using FEM, GIS, and Remote Sensing. *Journal of Waterway, Port, Coastal and Ocean Engineering-ASCE*, 137 (6), 286-299.

Singh, V. P. (1996). *Kinematic Wave Modeling in Water Resources: Surface-Water Hydrology*. Wiley and Sons, New York.

Singh, V. P. (2001). Kinematic wave modelling in water resources: a historical perspective. *Hydrological Processes*, 15 (4), 671-706.

Takayasu, H., Nishikawa, I. and Tasaki, H. (1988). Power-law mass distribution of aggregation systems with injection. *Physical Review A*, 37 (8), 3110-3117.

Velleux, M.L., England J.F. Jr. and Julien, P.Y. (2008). TREX: Spatially distributed model to assess watershed contaminant transport and fate. *Science of the Total Environment*, 404 (1), 113–128.

Viessman, W. and Lewis, L. (1995). *Introduction to Hydrology*. Fourth ed. Addison-Wesley Educational Publishers Inc. p. 760.

Vieux, B.E. and Vieux, J.E. (2002). VfloTM: A real-time distributed hydrologic model, in: *Proceedings of the 2nd Federal Interagency Hydrologic Modeling Conference*.

Wilson, J.P. (2012). Digital terrain modeling. *Geomorphology*, 137 (1), 107-121.

Wong, T.S.W. (1995). Time of concentration formulae for planes with upstream inflow. *Hydrological Sciences Journal*, 40 (5), 663-666.

Woolhiser, D.A. and Liggett, J.A. (1967). Unsteady, one-dimensional flow over a plane - The rising hydrograph. *Water Resources Research*, 3 (3), 753-771.

Woolhiser, D.A, Smith, R.E. and Goodrich, D.C. (1990). KINEROS: a kinematic runoff and erosion model: documentation and user manual. *USDA Agricultural Research Service*.

Xiong, Y.Y. and Melching, C.S. (2005). Comparison of kinematic-wave and nonlinear reservoir routing of urban watershed runoff. *Journal of Hydrologic Engineering*, 10 (1), 39-49.